# $^{113}$Cd Shielding Tensors of Monomeric Cadmium Compounds Containing Nitrogen Donor Atoms. 2. Syntheses, Crystal Structures, and $^{113}$Cd NMR Spectroscopy of the Six-Coordinate Complexes $[HB(pz)_3]_2Cd$, $[HB(3\text{-}Phpz)_3]_2Cd$, and $[B(pz)_4]Cd[HB(3\text{-}Phpz)_3]$ (pz = pyrazolyl)

**Daniel L. Reger,*,† Sheila M. Myers,† Scott S. Mason,†,‡ Donald J. Darensbourg,*,§ Matthew W. Holtcamp,§ Joseph H. Reibenspies,§ Andrew S. Lipton,|| and Paul D. Ellis*,||**

*Contribution from the Department of Chemistry and Biochemistry, University of South Carolina, Columbia, South Carolina 29208, Department of Chemistry, Texas A&M University, College Station, Texas 77843-3255, and Environmental Molecular Sciences Laboratory, Pacific Northwest Laboratory, P.O. Box 999, MS P7-55, Richland, Washington 99352*

*Received June 9, 1995*[⊗]

**Abstract:** All possible mixed-ligand complexes of the formula LL′Cd (L, L′ = $[HB(pz)_3]^-$, $[HB(3,5\text{-}Me_2pz)_3]^-$, $[B(pz)_4]^-$, $[HB(3\text{-}Phpz)_3]^-$ (pz = pyrazolyl)) were prepared by the reaction of a 1/1/1 molar ratio of the desired ligand salts and $CdCl_2$. The new symmetrical complex $[HB(3\text{-}Phpz)_3]_2Cd$ was prepared from 2 equiv of the ligand salt and $CdCl_2$. The solid state structures of $[HB(pz)_3]_2Cd$ (**1**), $[HB(3\text{-}Phpz)_3]_2Cd$ (**4**), and $[B(pz)_4]Cd[HB(3\text{-}Phpz)_3]$ (**10**) have been characterized by X-ray crystallography. All three are pseudo-octahedral, but the structures of both **4** and **10** are distorted by a rotational movement of one ligand relative to the other ligand. Because of this rotation with **4** and **10**, the *trans* N−Cd−N bond angles are significantly distorted from 180°, leading to one set of *cis*, interligand N−Cd−N angles that average 89.3 and 92.4° and another that average 100.6 and 105.7°, respectively. The Cd−N bond distances (average 2.33 Å) for **1** are similar to those observed earlier in the structures of $[HB(3,5\text{-}Me_2pz)_3]_2Cd$, $[B(pz)_4]_2Cd$ and $[B(3\text{-}Mepz)_4]_2Cd$, but the Cd−N distances are longer in **4** (average 2.39 Å) and in **10** ($[HB(3\text{-}Phpz)_3]^-$ ligand average 2.39 Å and the $[B(pz)_4]^-$ ligand 2.36 Å). The solution $^{113}$Cd NMR chemical shifts for complexes containing the $[HB(3\text{-}Phpz)_3]^-$ are substantially more shielded than the other complexes in the series. A regression analysis of the solution $^{113}$Cd NMR chemical shifts for all of these complexes for the shift caused by each ligand relative to $Cd(ClO_4)_2$ shows a good correlation of the calculated and observed chemical shifts of these complexes. These shift values (ligand/ligand shift, $\delta$) are $[HB(pz)_3]^-$/97.3, $[HB(3,5\text{-}Me_2pz)_3]^-$/101.7, $[B(pz)_4]^-$/107.4, and $[HB(3\text{-}Phpz)_3]^-$/44.9. The principal components of the $^{113}$Cd shielding tensor were determined from CP/MAS data. The $\sigma_{33}$ element was found to be relatively independent of the Cd−N bond lengths while the opposite is true of $\sigma_{11}$. This accounts for the dependence of the shielding anisotropies upon the bond distances. The respective chemical shift anisotropies and asymmetry parameters for **1** (both line shapes), **4**, and **10** are −238.7, −228.4, −138.5, and −220.8 ppm and 0.55, 0.65, 0.26, and 0.15 ppm.

## Introduction

We are interested in the preparation of cadmium coordination complexes in which the environment about the cadmium can be carefully controlled by choice of ligand. An important driving force for the development of this chemistry is the fact that cadmium has two important isotopes that are NMR active with spin quantum numbers of $I = {}^1/_2$. A number of research groups have been using $^{113}$Cd NMR as a "spin spy" in the study of zinc containing proteins.[1] The strategy here is to replace the zinc, a metal with few good spectroscopic handles, with cadmium and use NMR to explore the properties of the proteins. We are interested in the preparation of monomeric complexes in which the donor atom set can be controlled in a systematic manner to aid in the interpretation of both the solution and solid state NMR data on samples of biological interest. In addition, soluble cadmium carboxylate complexes containing the $[HB(3\text{-}Phpz)_3]^-$ ligand serve as excellent models for the more poorly characterized catalysts derived from zinc(II) dicarboxylates, of interest for the study of mechanistic aspects of $CO_2$/epoxide coupling processes.[2]

To achieve these goals, we have initiated an investigation into the preparation of complexes of cadmium(II) using the unique properties of the poly(pyrazolyl)borate ligand system.[3] These ligands are extremely versatile because substitution on the pyrazolyl rings can have a profound effect on the properties of the ligand. By preparing complexes containing two of the

† University of South Carolina.
‡ Present address: Department of Chemistry, Providence College, Providence, RI 02908.
§ Texas A&M University.
|| Pacific Northwest Laboratory.
⊗ Abstract published in *Advance ACS Abstracts*, October 1, 1995.

(1) (a) Summers, M. F. *Coord. Chem. Rev.* 1988, *86*, 43. (b) Coleman, J. E. In *Metallobiochemistry;* Riordan, J. F., Vallee, B. L., Eds.; Methods in Enzymology 227; Academic Press: San Diego, CA, 1993; Part D, pp 16−43.

(2) Darensbourg, D. J.; Holtcamp, M. W.; Khandelwal, B.; Klausmeyer, K. K.; Reibenspies, J. H. *J. Am. Chem. Soc.* **1995**, *117*, 538.

(3) (a) Trofimenko, S. *Acc. Chem. Res.* **1971**, *4*, 17. (b) Trofimenko, S. *J. Am. Chem. Soc.* **1967**, *89*, 3170. (c) Trofimenko, S. *J. Am. Chem. Soc.* **1967**, *89*, 6288. (d) Shaver, A. J. *Organomet. Chem. Lib.* **1976**, *3*, 157. (e) Trofimenko, S. *Prog. Inorg. Chem.* **1988**, *34*, 115. (f) Trofimenko, S.; *Chem. Rev.* **1993**, *93*, 943.

0002-7863/95/1517-10998$09.00/0 

tridentate poly(pyrazolyl)borate ligands, it was anticipated that the environment about the cadmium atom could be carefully controlled. The high steric bulk of the ligands should prevent any oligomerization or solvent coordination problems that have impacted on previous studies.[4]

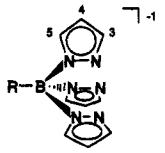

poly(pyrazolyl)borate ligands

The syntheses of the six-coordinate complexes $[HB(pz)_3]_2Cd$ (**1**), $[HB(3,5\text{-}Me_2pz)_3]_2Cd$ (**2**), $[B(3\text{-}Mepz)_4]_2Cd$, $[B(pz)_4]_2Cd$ (**3**) and $[HB(3,5\text{-}Me_2pz)_3]Cd[B(pz)_4]$ have been reported.[5] The solid-state structures of **2**, **3**, and $[B(3\text{-}Mepz)_4]_2Cd\cdot 2C_7H_8$ (**11**) were determined crystallographically.[5a] These three complexes have also been studied by CP/MAS solid state $^{113}Cd$ NMR.[6] The syntheses of the four-coordinate complexes $[H_2B(pz)_2]_2Cd$ and $[H_2B(3,5\text{-}Me_2pz)_2]_2Cd$ and five-coordinate $[HB(3,5\text{-}Me_2pz)_3]Cd[H_2B(pz)_2]$ were also reported.[5a] The six-coordinate complexes have a solution $^{113}Cd$ chemical shift range of 198.3–221.1 ppm. The four-coordinate complexes resonate at 298.7 and 303.3 ppm, respectively, and the five-coordinate complex at 225.1 ppm.

More recently, the chemistry of cadmium using the more bulky, "second generation" ligand[7] $[HB(3\text{-}Phpz)_3]^-$ has been investigated at both South Carolina and Texas A&M. The use of this ligand has allowed the syntheses of mixed-ligand complexes that have proven difficult to prepare using the $[HB(3,5\text{-}Me_2pz)_3]^-$ ligand.[2,8] As part of that work, the complex $[HB(3\text{-}Phpz)_3]_2Cd$ (**4**) was prepared and found to have a $^{113}Cd$ chemical shift that was very different from that of the six-coordinate complexes reported previously. Reported here are the solid state structures and CP/MAS solid state $^{113}Cd$ NMR investigations of **4**, the remaining symmetrical complex, **1**, of the series that had not been studied previously by these methods, and $[HB(3\text{-}Phpz)_3]Cd[B(pz)_4]$, a mixed-ligand complex. We also report the preparation and an analysis of the solution state $^{113}Cd$ NMR chemical shifts of all of the mixed-ligand complexes LL'Cd, where L and L' are $[HB(pz)_3]^-$, $[HB(3,5\text{-}Me_2pz)_3]^-$, $[B(pz)_4]^-$, and $[HB(3\text{-}Phpz)_3]^-$. Also presented are $^{113}Cd$ solution state NMR investigations of the chemical shifts of **4** as a function of temperature and concentration.

## Experimental Section

**General Procedure.** The $^1H$ NMR spectra were recorded on a Bruker AM300 or AM500 spectrometer using a broad-band probe. Proton chemical shifts are reported in parts per million vs internal $Me_4Si$. $^{113}Cd$ NMR spectra were recorded in $CDCl_3$ on a Bruker AM500 spectrometer using a 5-mm broad-band probe, and the chemical shifts are reported in parts per million vs external 0.1 M $Cd(ClO_4)_2$. In the assignment of $^1H$ NMR resonances, the following abbreviations are used: pz = pyrazolyl ring, $Me_2pz$ = 3,5-dimethylpyrazolyl ring, and Phpz = 3-phenylpyrazolyl ring. Mass spectral data were recorded on a Finnigan 4521 GC mass spectrometer or a VG 70SQ spectrometer using electron impact ionization. Clusters assigned to specific ions show appropriate isotopic patterns as calculated for the atoms present. The ligands of $K[HB(pz)_3]$,[9a] $K[HB(3,5\text{-}Me_2pz)_3]$,[9b] $K[B(pz)_4]$,[9a] and $K[HB(3\text{-}Phpz)_3]$[7a] were prepared according to published methods.

*Note! Cadmium compounds and their wastes are extremely toxic and must be handled carefully.*

**Bis[hydrotris(3-phenyl-1-pyrazolyl)borato]cadmium(II), $[HB(3\text{-}Phpz)_3]_2Cd$ (4).** $CdCl_2$ (0.18 g, 1.0 mmol) and $K[HB(3\text{-}Phpz)_3]$ (0.96 g, 2.0 mmol) were charged into a round bottom Schlenk flask. THF (40 mL) was added to the flask via syringe. The mixture was allowed to stir at room temperature for 4 h. The volatiles were removed in vacuo followed by a $CH_2Cl_2$ extraction. After removing the solvent, a white solid was isolated (0.72 g, 0.72 mmol, 72%), mp 196–197 °C. $^1H$ NMR ($CDCl_3$): $\delta$ 7.79 (6, d, $J$ = 2.0 Hz, 5-H (Phpz)), 6.98 (12, d, $J$ = 7.3 Hz, $C_6H_5$), 6.76 (6, t, $J$ = 7.3 Hz, $C_6H_5$), 6.47 (12, m, $C_6H_5$), 6.09 (6, d, $J$ = 2.0 Hz, 4-H (Phpz)). Mass spectrum: $m/z$ 996 ($M^+$). Anal. Calcd for $C_{54}H_{44}B_2N_{12}Cd$: C, 65.19; H, 4.46. Found: C, 65.13; H, 4.47.

**[Hydrotris(1-pyrazolyl)borato][hydrotris(3,5-dimethyl-1-pyrazolyl)borato] cadmium(II), $[HB(pz)_3]Cd[HB(3,5\text{-}Me_2pz)_3]$ (5).** $CdCl_2$ (0.18 g, 1.0 mmol), $K[HB(3,5\text{-}Me_2pz)_3]$ (0.35 g, 1.0 mmol), and $K[HB(pz)_3]$ (0.25 g, 1.0 mmol) were placed into a round bottom Schlenk flask. THF (40 mL) was added via syringe. The mixture was allowed to stir overnight at room temperature. The THF was evaporated, and the mixture was extracted with dichloromethane and then filtered. After removal of the dichloromethane, the residue was washed twice with toluene. The toluene was removed to give the desired white solid (0.10 g, 16%). $^1H$ NMR ($CDCl_3$): $\delta$ 7.73, 7.39 (3, 3, d, d; $J$ = 1.5 Hz, 3,5-H (pz)), 6.12 (3, t, $J$ = 2.0 Hz, 4-H (pz)), 5.67 (3, s, 4-H ($Me_2pz$)), 2.43, 1.57 (9, 9; s, s; 3,5-Me ($Me_2pz$)). Accurate mass spectrum ($m/z$) for $M^+$: calcd for $C_{24}H_{32}N_{12}{}^{11}B_2{}^{114}Cd$ 624.2093, found 624.2114.

**[Hydrotris(1-pyrazolyl)borato][tetrakis(1-pyrazolyl)borato]cadmium(II), $[HB(pz)_3]Cd[B(pz)_4]$ (6).** $CdCl_2$ (0.18 g, 1.0 mmol), $K[B(pz)_4]$ (0.31 g, 1.0 mmol), and $K[HB(pz)_3]$ (0.25 g, 1.0 mmol) were placed into a round bottom Schlenk flask. THF (40 mL) was added via syringe. The mixture was allowed to stir at room temperature overnight. THF was removed under vacuum. The product was then extracted with toluene and filtered. The toluene was removed to give a white solid (0.85 g). The $^1H$ NMR spectrum of this solid indicates the presence of a 20% impurity of $[HB(pz)_3]_2Cd$ that could not be removed. $^1H$ NMR ($CDCl_3$): $\delta$ 7.75, 7.36 (3, 3; d, d; $J$ = 2 Hz, 3,5-H $(pz)_3$), 7.50, 7.44 (4, 4; d, d; $J$ = 2 Hz, 3,5-H $(pz)_4$), 6.19 (4, t, $J$ = 2 Hz, 4-H $(pz)_4$), 6.15 (3, t, $J$ = 2 Hz, 4-H $(pz)_3$). Accurate mass spectrum ($m/z$) for $M^+$: calcd for $C_{21}H_{22}N_{14}{}^{11}B_2{}^{114}Cd$ 606.1372, found 606.1364.

**[Hydrotris(1-pyrazolyl)borato][hydrotris(3-phenyl-1-pyrazolyl)borato] cadmium(II), $[HB(pz)_3]Cd[HB(3\text{-}Phpz)_3]$ (7).** This compound was prepared in the same manner as prescribed for **5** (0.15 g, 20%). This compound was recrystallized from $CDCl_3$, mp 208–215 °C. $^1H$ NMR ($CDCl_3$): $\delta$ 7.89 (3, d, $J$ = 2.2 Hz, 5-H (Phpz)), 7.42, 6.77 (3, 3; d, d; $J$ = 1.8 Hz, 3,5-H (pz)), 7.10 (6, m, $C_6H_5$), 6.76 (3, m, $C_6H_5$), 6.47(3, d, $J$ = 2.2 Hz, 4-H (Phpz)), 6.52 (6, t, $J$ = 7.8 Hz, $C_6H_5$), 5.63 (3, t, $J$ = 2.0; 4-H (pz)). Accurate mass spectrum ($m/z$) for $M^+$: calcd for $C_{36}H_{32}N_{12}{}^{11}B_2{}^{114}Cd$ 768.2120, found 768.2093.

**[Hydrotris(3,5-dimethyl-1-pyrazolyl)borato][hydrotris(3-phenyl-1-pyrazolyl)borato]cadmium(II), $[HB(3,5\text{-}Me_2pz)_3]Cd[HB(3\text{-}Phpz)_3]$ (9).** $CdCl_2$(0.36 g, 2.0 mmol), $K[HB(3,5\text{-}Me_2pz)_3]$ (0.67 g, 2.0 mmol), and $K[HB(3\text{-}Phpz)_3]$ (0.96 g, 2.0 mmol) were placed into a round bottom Schlenk flask. THF (40 mL) was added via syringe. The mixture was allowed to stir at room temperature overnight. THF was removed under vacuum. The product was then extracted with toluene and filtered. The toluene was removed to give a white solid (0.85 g). The $^1H$ NMR spectrum of this solid indicates the presence of a 25%

(4) (a) Honkonen, R. S.; Doty, F. D.; Ellis, P. D. *J. Am. Chem. Soc.* **1983**, *105*, 4163. (b) Honkonen, R. S.; Ellis, P. D. *J. Am. Chem. Soc.* **1984**, *106*, 5488. (c) Honkonen, R. S.; Marchetti, P. S.; Ellis, P. D. *J. Am. Chem. Soc.* **1986**, *108*, 912. (d) Marchetti, P. S.; Honkonen, R. S.; Ellis, P. D. *J. Magn. Res.* **1987**, *71*, 294. (e) Kennedy, M. A.; Ellis, P. D. *Inorg. Chem. Soc.* **1990**, *29*, 541. (f) Kennedy, M. A.; Ellis, P. D.; Jakobsen, H. J. *Inorg. Chem.* **1990**, *29*, 550. (g) Rivera, E.; Ellis, P. D. *Inorg. Chem.* **1992**, *31*, 2096. (h) Rivera, E.; Kennedy, M. A.; Adams, R. D.; Ellis, P. D. *J. Am. Chem. Soc.* **1990**, *112*, 1400.

(5) (a) Reger, D. L.; Mason, S. S.; Rheingold, A. L.; Ostrander, R. L. *Inorg. Chem.* **1993**, *32*, 5216. (b) Trofimenko, S. *J. Am. Chem. Soc.* **1967**, *89*, 3170.

(6) Lipton, A. S.; Mason, S. S.; Reger, D. L.; Ellis, P. D. *J. Am. Chem. Soc.* **1994**, *116*, 10182.

(7) (a) Trofimenko, S.; Calabrese, J. C.; Thompson, J. S. *Inorg. Chem.* **1987**, *26*, 1507. (b) Trofimenko, S.; Calabrese, J. C.; Domaille, P. J.; Thompson, J. S. *Inorg. Chem.* **1989**, *28*, 1091.

(8) (a) Reger, D. L. Myers, S. M.; Mason, S. S.; Rheingold, A. L.; Haggerty, B. S.; Ellis, P. D. *Inorg. Chem.*, in press. (b) Reibenspies, J. H.; Holtcamp, M. W.; Khandelwal, B.; Darensbourg, D. J. *Z. Kristallogr.*, in press.

(9) (a) Trofimenko, S. *J. Am. Chem. Soc.* **1967**, *89*, 3170. (b) Trofimenko, S. *J. Am. Chem. Soc.* **1967**, *89*, 6288.

impurity of both $L_2Cd$ complexes that could not be removed. $^1H$ NMR ($CDCl_3$): $\delta$ 7.87 (3, m, 5-H (Phpz)), 7.41−7.16 (15, m, $C_6H_5$), 6.10 (3, d, $J$ = 2.2, 4-H (Phpz)), 5.23 (3, s, 4-H ($Me_2pz$)), 2.45, 1.17 (6, 6; s, s; $CH_3$). Accurate mass spectrum ($m/z$) for $M^+$ − 3,5-$Me_2pz$: calcd for $C_{37}H_{37}N_{10}{}^{11}B_2{}^{114}Cd$ 757.2422, found 757.2413. The high-resolution mass spectrum could not be reported for $M^+$ at 852 because a daughter ion of the $[HB(3\text{-}Phpz)_3]_2Cd$ impurity matches this value.

**[Hydrotris(3-phenyl-1-pyrazolyl)borato][tetrakis(1-pyrazolyl)-borato] cadmium(II), $[B(pz)_4]Cd[HB(3\text{-}Phpz)_3]$ (10).** $CdCl_2$ (0.36 g, 2.0 mmol), $K[B(pz)_4]$ (0.62 g, 2.0 mmol), and $K[HB(3\text{-}Phpz)_3]$ (0.96 g, 2.0 mmol) were placed into a round bottom Schlenk flask. THF (50 mL) was added via syringe. The mixture was allowed to stir at room temperature overnight. THF was removed under vacuum. The product was then extracted with toluene and filtered twice. The toluene was removed to give a white solid. This solid was crystallized from $CH_2Cl_2$. The crystals were then washed with $CH_2Cl_2$ to give pure **10** (0.93 g, 56%), mp 190−191 °C. $^1H$ NMR ($CDCl_3$): $\delta$ 7.91 (3, d, $J$ = 2.2 Hz, 5-H (Phpz)), 7.47 (4, br, (pz)), 7.11−6.55 (19, m , pz and $C_6H_5$), 6.48 (3, d, $J$ = 2.2 Hz, 4-H (Phpz)), 5.84 (3, br, 4-H (pz)). $^1H$ NMR ($CD_2Cl_2$, −51 °C): $\delta$ 7.95, 7.71 (1, 1; s, s; 3,5-H (pz)), 7.93 (3, d, $J$ = 2.1 Hz , 5-H (Phpz)), 7.31 (3, d, $J$ = 2.1 Hz, 3-H (pz)), 7.04 (6, d, $J$ = 7.2 Hz, $C_6H_5$), 6.82 (3, d, $J$ = 2.1 Hz, 5-H (pz)), 6.79 (3, t, $J$ = 7.5 Hz, $C_6H_5$), 6.55 (6, t, $J$ = 7.7 Hz, $C_6H_5$), 6.50 (1, s, 4-H(pz)), 6.48 (3, d , $J$ = 2.2 Hz, 4-H (Phpz)), 5.63 (2, s, 4-H (pz)). Accurate mass spectrum ($m/z$) for $M^+$: calcd for $C_{39}H_{34}N_{14}{}^{11}B_2{}^{114}Cd$ 834.2311, found 834.2302.

**Solid State $^{113}Cd$ NMR.** The solid state NMR spectra were acquired utilizing either a Varian UNITY$^{plus}$ spectrometer with a widebore Oxford Instruments magnet operating at 7.05 T (Larmor frequency of 300 MHz for $^1H$ and 66.546 MHz for $^{113}Cd$) or 11.7 T (500 MHz for $^1H$ and 110.78 MHz for $^{113}Cd$). The samples were ground and packed into silicon nitride rotors with vespel end caps for use in a 7-mm supersonic probe from Doty Scientific Inc. Spinning speeds were regulated by a Doty Scientific Inc. spin rate controller. All chemical shifts and tensor elements are referenced to an external sample of 0.1 M $Cd(ClO_4)_2$ in a 1:1 $H_2O/D_2O$ solution at 25 °C, with positive shifts denoting movement of resonances to lower shielding.

The pulse sequence used was a standard single contact cross polarization (CP) sequence with proton decoupling.[10] The recycle delay used was 20 s with a $^1H$ $\pi/2$ pulse width of 5.5 $\mu$s and a contact time of 6 ms for all samples. Principle elements of the shielding tensor were extracted from the CP/MAS data utilizing either a SIMPLEX or MINPACK algorithm to optimize the asymmetry parameter and two of the three tensor values with a program run on a Silicon Graphics ONYX.[11] The calculations assumed no couplings (neither dipolar nor scalar).

**X-ray Crystallographic Study of 1 and 10.** Crystal data and details of data collection are given in Table 1. The details of the crystallography for **4** have been deposited elsewhere.[12] Colorless crystals of **1** (0.2 × 0.2 × 0.2 mm) were grown from $CH_2Cl_2$/hexane, and of **10** (0.3 × 0.3 × 0.1 mm) by evaporation of a $CH_2Cl_2$ solution, and were mounted in a capillary tube at room temperature. Preliminary examinations and data collections were performed on a Rigaku AFC5R X-ray diffractometer (oriented graphite monochromator Mo K$\alpha$ = 0.710 73). Cell parameters were calculated from the least squares fitting of the setting angles for 25 reflections. $\omega$ scans for several intense reflections indicated acceptable crystal quality. Data were collected for 5.0° < $2\theta$ < 50.0° at 293 K. Three control reflections collected every 150 reflections showed no significant trends. Background measurements were performed by stationary crystal and stationary counter techniques at the beginning and end of each scan for one-half of the total scan time. Lorentz and polarization corrections were applied to 4246 for **1** and 4123 reflections for **10**. No absorption correction was applied to **1** and a Difabs absorption correction was applied to **10**. Totals of 4116 unique reflections ($R_{int}$ = 0.0761) for **1** and 2253 unique reflections for **10**, with $|I| > 2.0\sigma I$, were used in further calculations. The structures were solved by direct methods [SHELXS, SHELXTL-Plus program package, Sheldrick (1993)]. Hydrogen atoms were placed in idealized positions with isotropic thermal parameters fixed at 0.08 Å$^2$. Neutral-atom scattering factors were taken from the *International Tables for X-ray Crystallography*. One molecule of $CH_2Cl_2$ per molecule of **10** was located in that structure (verified by NMR). The atoms Cl1, Cl2, and C40 were located with 81% partial occupancy.

**Table 1.** Crystallographic Data for Complexes **1** and **10**

| | **1** | **10** |
|---|---|---|
| emp form | $C_{18}H_{20}B_2CdN_{12}$ | $C_{40}H_{36}B_2CdCl_2N_{14}$ |
| fw | 538.48 | 917.75 |
| space group | $C2/c$ | $P2_1P2_1P2_1$ |
| $V$, Å$^3$ | 4673.4(1) | 4199(4) |
| $Z$ | 8 | 4 |
| $D_{calcd}$, g/cm$^3$ | 1.531 | 1.452 |
| $a$, Å | 19.132(2) | 12.672(8) |
| $b$, Å | 13.653(2) | 15.894(8) |
| $c$, Å | 19.177(2) | 20.851(11) |
| $\alpha$, deg | 90 | 90 |
| $\beta$, deg | 111.10(1) | 90 |
| $\gamma$, deg | 90 | 90 |
| $T$, K | 293 | 293(2) |
| $\mu$(Mo K$\alpha$), mm$^{-1}$ | 0.967 | 0.696 |
| wavelength, Å | 0.71073 | 0.71073 |
| $R_F$, %[a] | 4.84 | 7.35 |
| $R_{wF}$, %[a] | 8.69 | 16.62 |

[a] $R_F = \Sigma|F_o - F_c|/\Sigma F_o$ and $R_{wF} = \{[\Sigma w(F_o^2 - F_c^2)^2]/[\Sigma wF_o^2)^2]\}^{1/2}$. $S$ = 1.044 and 1.055, respectively, for **1** and **10**.

## Results

**Syntheses of Complexes.** All possible mixed-ligand complexes of the formula LL'Cd (L, L' = $[HB(pz)_3]^-$, $[HB(3,5\text{-}Me_2pz)_3]^-$, $[B(pz)_4]^-$, $[HB(3\text{-}Phpz)_3]^-$) were prepared by the reaction of a 1/1/1 molar ratio of the desired ligand salts and $CdCl_2$ (eq 1, note that two pyrazolyl rings have been omitted

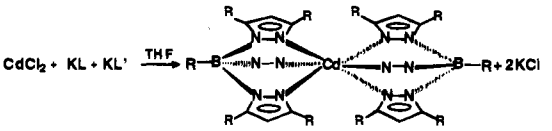


(1)

L = L' = $[HB(3\text{-}Phpz)_3]^-$ (**4**)
L = $[HB(pz)_3]^-$, L' = $[HB(3,5\text{-}Me_2pz)_3]^-$ (**5**)
L = $[HB(pz)_3]^-$, L' = $[B(pz)_4]^-$ (**6**)
L = $[HB(pz)_3]^-$, L' = $[HB(3\text{-}Phpz)_3]^-$ (**7**)
L = $[HB(3,5\text{-}Me_2pz)_3]^-$, L' = $[B(pz)_4]^-$ (**8**)
L = $[HB(3,5\text{-}Me_2pz)_3]^-$, L' = $[HB(3\text{-}Phpz)_3]^-$ (**9**)
L = $[B(pz)_4]^-$, L' = $[HB(3\text{-}Phpz)_3]^-$ (**10**)

for clarity). The new symmetrical complex $[HB(3\text{-}Phpz)_3]_2Cd$ was prepared from 2 equiv of the ligand salt and $CdCl_2$. In the mixed-ligand syntheses, some of the symmetrical $L_2Cd$ complexes also formed. For **6** and **9**, it did not prove possible to completely separate these impurities, but the new complexes were definitively characterized by NMR spectroscopy and high-resolution mass spectrometry. Complex **8** was reported previously.[5a]

These cadmium complexes are air stable in both the solid and solution phase. They are soluble in aromatic or halocarbon solvents but only sparingly soluble in hydrocarbons. In complex **6**, the pyrazolyl rings of the $[B(pz)_4]^-$ ligand are equivalent in the $^1H$ NMR spectrum, even at low temperature, but in **10**, the resonances appear in the expected 3/1 ratio at low temperatures.

**Solid State Structures of $[HB(pz)_3]_2Cd$ (1), $[HB(3\text{-}Phpz)_3]_2Cd$ (4), and $[B(pz)_4]Cd[HB(3\text{-}Phpz)_3]$ (10). $[HB(pz)_3]_2Cd$.** There are two independent molecules in the lattice

(10) (a) Hartman, S. R.; Hahn, E. L. *Phys. Rev.* **1962**, *128*, 2024. (b) Pines, A.; Gibby, M. G.; Waugh, J. S. *J. Chem. Phys.* **1972**, *56*, 1776. (c) Pines, A.; Gibby, M. G.; Waugh, J. S. *J. Chem. Phys.* **1973**, *59*, 569.

(11) Koons, J. M.; Hughes, E.; Ellis, P. D. *Anal. Chim. Acta* **1993**, *283*, 1045.

(12) (a) Reibenspies, J. H.; Klausmeyer, K. K.; Niezgoda, S. A.; Holtcamp, M. W.; Khandelwal, B.; Darensbourg, D. J. *Z. Kristallogr.*, in press. (b) Sheldrick, G. M. *SHELXS-93 User Guides*; Crystallographic Department, University of Gottingen: Gottingen, Germany, 1993. (c) *International Tables for X-Ray Crystallography*: Kynoch Press: Birmingham, England, 1974.

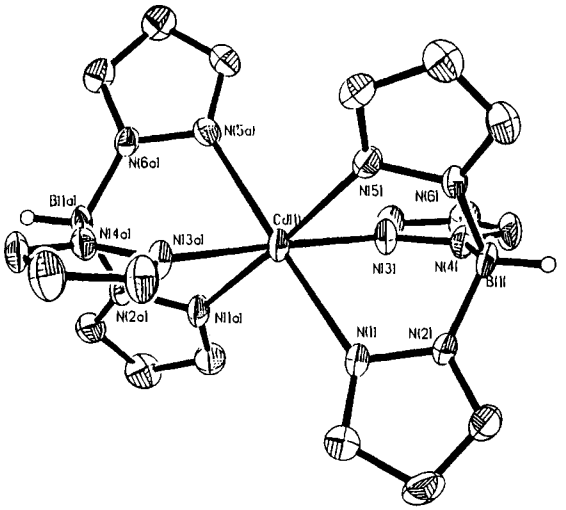


**Figure 1.** ORTEP diagram of one molecule of $[HB(pz)_3]_2Cd$ (**1**).

**Table 2.** Selected Bond Distances and Bond Angles for $[HB(pz)_3]_2Cd$ (**1**), $[HB(3\text{-}Phpz)_3]_2Cd$ (**4**), and $[B(pz)_4]Cd[HB(3\text{-}Phpz)_3]$ (**10**)

| | **1** | **4** | **10** |
|---|---|---|---|
| | Bond Distances (Å) | | |
| Cd−N(1) | 2.341(6) | 2.389(6) | 2.380(11) |
| Cd−N(3) | 2.282(5) | 2.415(6) | 2.411(10) |
| Cd−N(5) | 2.357(6) | 2.351(6) | 2.392(11) |
| Cd−N(7) | 2.355(6) | | 2.313(11) |
| Cd−N(9) | 2.293(6) | | 2.397(11) |
| Cd−N(11) | 2.371(6) | | 2.369(10) |
| | Bond Angles (deg) | | |
| N(1)−Cd−N(3) | 83.4(2) | 84.23(2) | 81.5(4) |
| N(1)−Cd−N(5) | 78.9(2) | 85.57(2) | 81.5(4) |
| N(3)−Cd−N(5) | 83.8(2) | 85.76(2) | 84.3(4) |
| N(7)−Cd−N(9) | 83.5(2) | | 80.6(4) |
| N(7)−Cd−N(11) | 78.2(2) | | 81.1(4) |
| N(9)−Cd−N(11) | 83.2(2) | | 79.6(4) |
| N(1)−Cd−N(5a, 3a, or 7) | 176.3(3) | 170.4(2) | 167.2(4) |
| N(3)−Cd−N(3a, 1a, or 9) | 178.0(3) | 170.4(2) | 168.0(4) |
| N(5)−Cd−N(1a, 5a, or 11) | 176.3(3) | 172.3(4) | 171.6(4) |
| N(1)−Cd−N(1a, 5a, or 9) | 104.6(3) | 99.3(2) | 110.4(4) |
| N(1)−Cd−N(3a, 1a, or 11) | 95.4(2) | 85.2(3) | 94.2(4) |
| N(3)−Cd−N(1a, 5a, or 7) | 95.4(2) | 91.4(2) | 87.9(4) |
| N(3)−Cd−N(5a, 3a, or 11) | 97.6(2) | 103.2(3) | 102.3(4) |
| N(5)−Cd−N(3a, 1a, or 7) | 97.6(2) | 99.3(2) | 104.5(4) |
| N(5)−Cd−N(5a, 3a, or 9) | 97.7(3) | 91.4(2) | 95.1(4) |

of complex **1**, each of which has 2-fold rotational symmetry. An ORTEP diagram of one molecule of **1** is shown in Figure 1, and both molecules are shown showing their relative orientation and the complete numbering scheme in the supporting information. Important bond angles and distances are listed in Table 2.

The structure is six-coordinate with a pseudo-octahedral arrangement of the nitrogen donor atoms about the cadmium atom. The chelate rings restrain the intraligand N−Cd−N bond angles to an average of 81.8°, but the *trans* N−Cd−N bond angles are close to 180°. The Cd−N bond distances vary from 2.282(5) to 2.371(6) Å. The average of 2.33 Å is very similar to the averages of these distances in the structures of $[HB(3,5\text{-}Me_2pz)_3]_2Cd$ (**2**), $[B(pz)_4]_2Cd$ (**3**), and $[HB(3\text{-}Mepz)_3]_2Cd$ (**11**) of 2.35, 2.33, and 2.34 Å, respectively.[5a] The bond angles are also similar in the four structures. For example, the *cis* interligand N−Cd−N bond angles average 98.1° and the N−B−N bond angles average 110.0° in the structure of **1**, both the same as the average of these angles in the structures of **2**, **3**, and **11**.

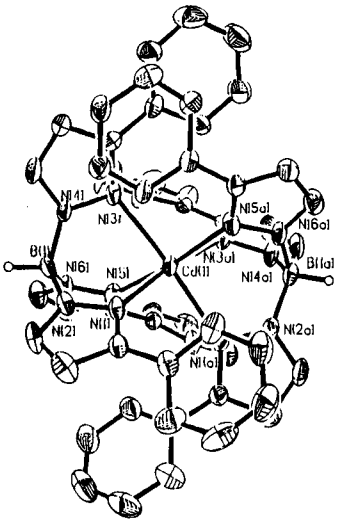


**Figure 2.** ORTEP diagram of $[HB(3\text{-}Phpz)_3]_2Cd$ (**4**).

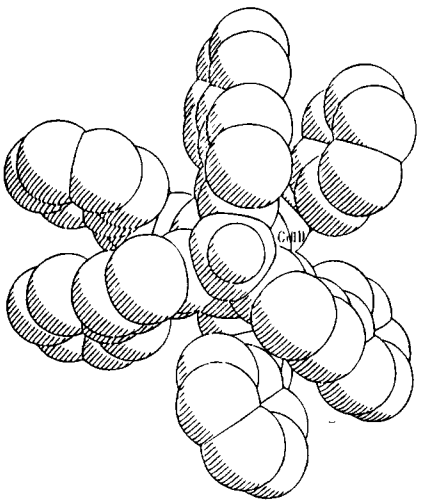


**Figure 3.** Space filling drawing of $[HB(3\text{-}Phpz)_3]_2Cd$ (**4**).

**$[HB(3\text{-}Phpz)_3]_2Cd$.** An ORTEP diagram of **4** is shown in Figure 2 and a space filling drawing oriented down the B···Cd···B axis is shown in Figure 3. Important bond angles and distances are listed in Table 2. In the pseudo-octahedral structure, the phenyl substituents of one ligand fit between the pyrazolyl rings of the other, but clearly, the structure is more crowded than those of **1**, **2**, **3**, and **11**. This crowding is reflected by an increase in the Cd−N bond distances in the latter four structures from the average of 2.34 Å to an average of 2.39 Å in **4**. To accommodate the longer Cd−N bonds, the N−B−N angles average 111.6°, 1.8° larger than the average of the other four complexes. This change causes the average intraligand N···N nonbonding distance for the donor atoms to increase from an average of 3.06 (range = 2.979−3.098) Å in **1** to 3.24 (range = 3.184−3.274) Å in **4**.

The phenyl rings rotate in the range 9.6−31.3° relative to the planes of the pyrazolyl rings. Rotation of the phenyl groups relieves unfavorable intraligand interaction of the *ortho* hydrogen atoms with the pyrazolyl ring to which it is bonded. The importance of this rotation is highlighted in the structure of a complex containing the mesityl (Ms) analog of $[HB(3\text{-}Phpz)_3]^-$, $[HB(3\text{-}Mspz)_3]Mo(CO)_2(\eta^3\text{-}CH_2CMeCH_2)$.[13] In this complex the *ortho* methyl groups on the mesityl rings force a nearly

(13) Rheingold, A. L.; White, C. B.; Trofimenko, S. *Inorg. Chem.* **1993**, *32*, 3471.
(14) Frazer, A.; Piggott, B.; Hursthouse, M. B.; Mazid, M. *J. Am. Chem. Soc.* **1994**, *116*, 4127.

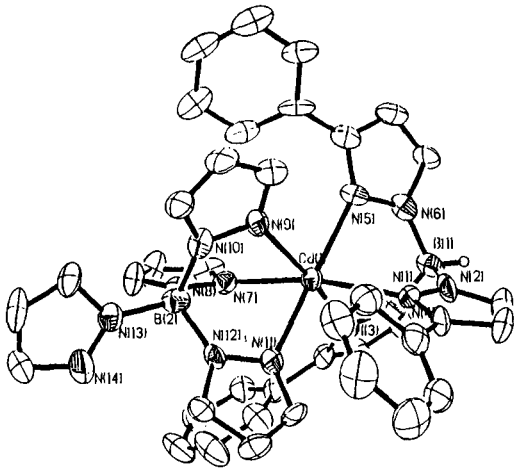


**Figure 4.** ORTEP diagram of $[B(pz)_4]Cd[HB(3\text{-}Phpz)_3]$ (**10**).

perpendicular orientation relative to the pyrazolyl ring to which they are bonded. As shown best in Figure 3, the rotation of the phenyl rings in **4** is restrained by interligand interactions. These restraints are also evident in comparisons to other structures containing this ligand and the structure of **10** discussed below. This rotation angle is 49° in $[HB(3\text{-}Phpz)_3]In$[14] and ranges from 32 to 37° in $[HB(3\text{-}Phpz)_3]CoNCS$.[7a] In the former complex, there are no other ligands present, and in the latter, only a small second ligand is present. In $[HB(3\text{-}Phpz)_3]_2Fe$, a molecule like **4**, the angles range from 23 to 31°.[15]

Figure 3 shows that the interligand pyrazolyl rings and attached phenyl groups are arranged in three pairs where the pyrazolyl and phenyl aromatic rings are stacked over each other. This stacking is also seen in the top of Figure 2, where the phenyl groups attached to the pyrazolyl ring containing the N(5a) donor atom are viewed on top of the pyrazolyl ring containing the N(3) donor atom. This arrangement is caused by a rotation of one ligand relative to the other so as to lower "paired" interligand N−Cd−N angles, such as N(3)−Cd−N(5a), to an average of 89.3° and to increase ones between pairs, such as N(3)−Cd−N(3a), to an average of 100.6°. The analogous angles in the structures of **1**, **2**, **3**, and **11** are much more regular.

**$[B(pz)_4]Cd[HB(3\text{-}Phpz)_3]\cdot CH_2Cl_2$.** An ORTEP diagram of **10** is shown in Figure 4, and important bond angles and distances are listed in Table 2. This structure represents one of the first mixed poly(pyrazolyl)borate complexes to be reported, and the first for relatively nonbulky poly(pyrazolyl)-borate ligands. Trofimenko and co-workers have reported complexes of this type of the first row transition metals in the +2 oxidation state using the bulky $[HB(3\text{-}Pr^i\text{-}4\text{-}Brpz)_3]^-$ ligand.[16] The structure of **10** is particularly novel because we have also structurally characterized both analogous homoleptic derivatives, $[B(pz)_4]_2Cd$ (**3**)[5a] and $[HB(3\text{-}Phpz)_3]_2Cd$ (**4**).

The structure of **10** is fairly similar to one-half each of the structures of **3** and **4**. The average Cd−N bond distance of the $[HB(3\text{-}Phpz)_3]^-$ ligand in **10** is 2.39 Å, the same as in **4**. The phenyl rings rotate in the range 38.1−44.5° relative to the planes of the pyrazolyl rings. This rotation is substantially larger than in **4**, as expected, because of the decrease in interligand repulsions. The average intraligand N···N nonbonding distance for the donor atoms of the $[HB(3\text{-}Phpz)_3]^-$ ligand is 3.16 Å, 0.08 Å less than observed with **4**.

The average Cd−N bond distance of the $[B(pz)_4]^-$ ligand is longer in **10** (2.36 Å) than in **3** (2.33 Å), but the pattern observed in **3** of one short and two longer Cd−N bonds (2.308(8), 2.362(8), 2.365(8) Å and 2.313(11), 2.369(10), 2.397(11) Å for **10**) is preserved. Given the presence of the bulky $[HB(3\text{-}Phpz)_3]^-$ ligand, the longer distances in the $[B(pz)_4]^-$ ligand of **10** are expected, but the very long Cd−N(11) distance of 2.397(11) is surprising given that this bond is longer than two of the three bonds formed by the more bulky $[HB(3\text{-}Phpz)_3]^-$ ligand. The average intraligand N···N nonbonding distance for the donor atoms of the $[B(pz)_4]^-$ ligand is 3.05 Å, 0.03 Å longer than in **3**. These nonbonding distances are the largest "bite" distances that have been reported for a *tridentate* $[B(pz)_4]^-$ ligand. As discussed previously by some of us[17] and more quantitatively by Sohrin,[18] intraligand contacts become substantial for the $[B(pz)_4]^-$ ligand if the "bite" distances are above 3.0 Å.

The rotational distortion of one ligand relative to the other ligand noted for **4** is also observed for **10**. The *trans* N−Cd−N bond angles are significantly distorted from 180°, leading to one set of *cis* interligand N−Cd−N angles that average 92.4° and another that average 105.7°.

**Table 3.** Measured and Predicted $^{113}Cd$ NMR Chemical Shifts (ppm vs $Cd(ClO_4)_2$)

| | measured signal | predicted signal |
|---|---|---|
| $[HB(pz)_3]_2Cd$ (**1**) | 198.3 | 194.5 |
| $[HB(3,5\text{-}Me_2pz)_3]_2Cd$ (**2**) | 201.9 | 203.4 |
| $[B(pz)_4]_2Cd$ (**3**) | 221.1 | 214.8 |
| $[HB(3\text{-}Phpz)_3]_2Cd$ (**4**) | 94.0 | 89.7 |
| $[HB(pz)_3]Cd[HB(3,5\text{-}Me_2pz)_3]$ (**5**) | 201.2 | 198.9 |
| $[HB(pz)_3]Cd[B(pz)_4]$ (**6**) | 198.2 | 204.6 |
| $[HB(pz)_3]Cd[HB(3\text{-}Phpz)_3]$ (**7**) | 138.8 | 142.1 |
| $[HB(3,5\text{-}Me_2pz)_3]Cd[B(pz)_4]$ (**8**) | 209.0 | 209.1 |
| $[HB(3,5\text{-}Me_2pz)_3]Cd[HB(3\text{-}Phpz)_3]$ (**9**) | 147.5 | 146.6 |
| $[B(pz)_4]Cd[HB(3\text{-}Phpz)_3]$ (**10**) | 146.2 | 152.3 |

**Table 4.** Chemical Shift in LL'Cd Complexes (ppm) Caused by Each Ligand Calculated versus the $Cd(ClO_4)_2$ Standard

| ligand | $[HB(pz)_3]^-$ | $[HB(3,5\text{-}Me_2pz)_3]^-$ | $[B(pz)_4]^-$ | $[HB(3\text{-}Phpz)_3]^-$ |
|---|---|---|---|---|
| ligand shift | 97.3 | 101.7 | 107.4 | 44.9 |

**Solution $^{113}Cd$ NMR Results.** Table 3 lists the $^{113}Cd$ NMR chemical shifts for all of the six-coordinate complexes of the general formula $[poly(pyrazolyl)borate]_2Cd$ that have been prepared with the four ligands studied here. Although we were initially surprised by the location of the highly shielded resonance for **4** in comparison to those of the other homoleptic complexes, mixed-ligand complexes of the $[HB(3\text{-}Phpz)_3]^-$ ligand are also more shielded than complexes of the other ligands reported here. Also shown in Table 3 are the shifts predicted on the basis of a regression analysis of the data. In this analysis, the shift caused by each ligand is relative to $Cd(ClO_4)_2$ assigned as 0 ppm. These shifts are shown in Table 4. In the analysis, the value of $R^2$ is 0.989 and the error on the shift values in Table 4 is ± 2. Figure 5 shows a plot of the predicted versus observed values. Clearly there is a good correlation of the calculated and observed chemical shifts of these complexes. Complexes containing the $[B(pz)_4]^-$ ligand vary the most from the predicted value.

Figure 6 shows a plot of the $^{113}Cd$ chemical shift of **4** versus temperature. A smooth shielding variation of 8 ppm is observed as the temperature is lowered from 25 to −51 °C. The effect of concentration on $^{113}Cd$ chemical shift of **4** was also studied

(15) Eichhorn, D. M.; Armstrong, W. H. *Inorg. Chem.* **1990**, *29*, 3607.
(16) Calabrese, J. C.; Domaille, P. J.; Thompson, J. S.; Trofimenko, S. *Inorg. Chem.* **1990**, *29*, 4429.
(17) Reger, D. L.; Huff, M. F.; Rheingold, A. L.; Haggerty, B. S. *J. Am. Chem. Soc.* **1992**, *114*, 579.
(18) (a) Sohrin, Y.; Matsui, M.; Hata, Y.; Hasegawa, H.; Kokusen, H *Inorg. Chem.* **1994**, *33*, 4376. (b) Sohrin, Y.; Kokusen, H; Kihara, S.; Matsui, M.; Kushi, Y.; Shiro, M. *J. Am. Chem. Soc.* **1993**, *115*, 4128.

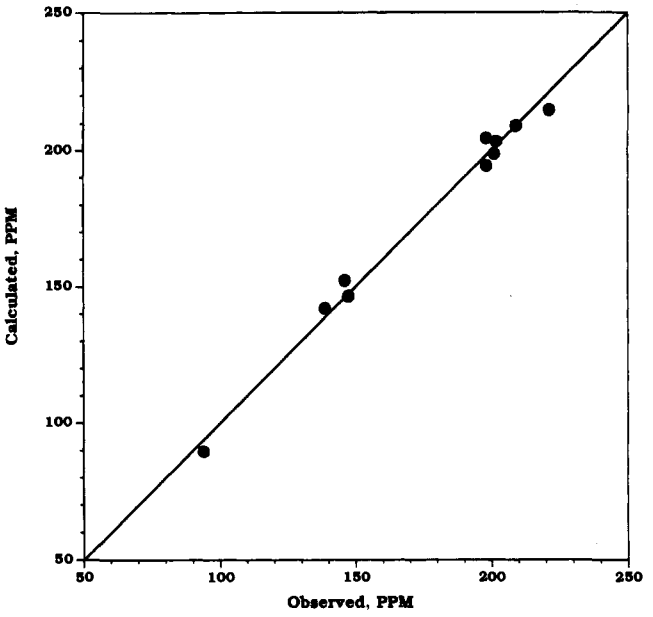


**Figure 5.** Plot of the predicted versus observed values of the solution $^{113}Cd$ NMR chemical shifts for **1**−**10**.

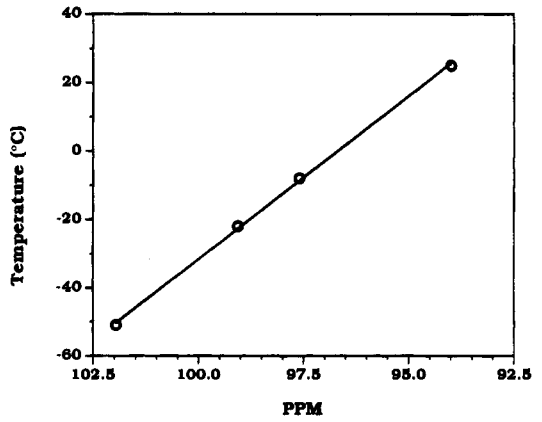


**Figure 6.** $^{113}Cd$ NMR chemical shift of **10** in solution as a function of temperature.

and found to vary only from 93.8 to 94.1 ppm when the concentration changed from 0.019 to 0.062 M.

**Solid State $^{113}Cd$ NMR Results.** The principal components of the shielding tensors of each of the six-coordinate complexes are listed in Table 5. Also tabulated are the chemical shift anisotropy (CSA, $\Delta\sigma$) and the asymmetry parameter, $\eta$. The designation of the two forms of $[HB(pz)_3]_2Cd$ will be **1a** and **1b** for convenience. Structure **1a** refers to the complex that has an average Cd−N bond distance of 2.327 Å, while **1b** refers to the structure that has an average Cd−N distance of 2.340 Å.

Figure 7 depicts the CP/MAS spectrum of complex **1** (**a** and **b**) and the simulated spectrum calculated from both sets of shielding tensor data at two spinning speeds. The respective isotropic shifts in the solid state are 207.6 and 177.9 ppm. The value of $\eta$ and the CSA extracted for **1a** are 0.56 and −238.7 ppm, and those of **1b** are 0.65 and −228.4 ppm, respectively. Neither of the overlapping line shapes contains any resolvable coupling; however, the presence of *J*-coupling from the $^{14}N$'s to the $^{113}Cd$ is suspected from the line widths of the sidebands of the MAS line shapes. The only six-coordinate pyrazolylborate complex to have resolved couplings has been $[HB(3,5\text{-}Me_2pz)_3]_2Cd$, in which all of the nitrogens are equivalent. The resulting line width of the sidebands is simulated using mostly Gaussian line broadening in addition to some Lorentzian broadening.

For complex **4**, the isotropic shift in the solid state is 89.3 ppm and the values of $\eta$ and $\Delta\sigma$ are 0.26 and −138.5 ppm, respectively. Due to the small anisotropy, the spinning speeds used were kept lower to maintain the chemical shift information in the spinning sidebands. The solid state shift of the mixed-ligand complex, **10**, is 134.0 ppm with an $\eta$ value of 0.15 and a $\Delta\sigma$ of −220.8 ppm. The spectra of **10** show impurities arising from the respective homoleptic compounds that could not be removed. The CP/MAS spectra of **4** and **10** and the resulting simulations are included in the supporting information.

## Discussion

**Coordination Geometries.** The structures of **1**−**4**, **10**, and **11** represent the first extensive series of analogous structures to be carried out containing different poly(pyrazolyl)borate ligands coordinated to the same central metal atom. In iron chemistry, the structures of $[HB(pz)_3]_2Fe$ (**12**),[19] $[B(pz)_4]_2Fe$ (**13**),[20] $[HB(3,5\text{-}Me_2pz)_3]_2Fe$ (**14**)[19] and $[HB(3\text{-}Phpz)_3]_2Fe$ (**15**)[15] have been determined. The average N−Fe−N bond distances in the four complexes change from 1.97 (both **12** and **13**) to 2.17 to 2.25 Å, respectively, a much greater change than observed with cadmium. The change in going from **12** and **13** to **14** is influenced by a change in the spin state of the iron from low spin to high spin, an effect not relevant to the cadmium structures. The change between **14** and **15** of 0.08 Å is slightly larger than going from **1** to **4** of 0.06 Å. The similarity in the structural parameters of **1**, **2**, **3**, and **11** and the lesser change in the structure of **4** when compared to the iron structures is explained by a reduction in interligand repulsions because of the larger radius of cadmium.[21]

It is also of interest to compare these structures to those of $[HB(3,5\text{-}Me_2pz)_3]_2Zn$ (**16**)[22] and $[HB(3\text{-}Phpz)_3]_2Zn$ (**17**).[23] For **16**, the structure is six-coordinate, but for **17** the two ligands are only bidentate, leading to a four-coordinate structure. The average M−N bond distance increases by 0.18 Å in **2** when compared to **16**, indicating that the larger cadmium atom can more readily accommodate two tridentate, poly(pyrazolyl)borate ligands substituted at the 3-position.

The changes in bond lengths in any of these structures clearly do not correlate with the basicity of the ligands, as measured by their first acid dissociation constant. These $pK_a$ values are 6.92 for $[HB(pz)_3]^-$, 10.12 for $[HB(3,5\text{-}Me_2pz)_3]^-$, 6.06 for $[B(pz)_4]^-$ in water,[18] and 8.8 for $[HB(3\text{-}Phpz)_3]^-$ in 30% dioxane in water.[24]

**$^{113}Cd$ Chemical Shifts.** The concept of chemical shift additivity is not a new one. There are an ever increasing number of tables of additivity constants to allow the estimation of the contribution of different environments to the chemical shift. Some of the earliest tables are "Shoolery's effective shielding constants",[25] which permit calculation of a proton chemical shift of a methylene group attached to two functional groups. There are other examples for $^{13}C$ NMR[26] as well as $^{15}N$ additivity relationships.[27]

(19) Oliver, J. D.; Mullica, D. F.; Hutchinson, B. B.; Milligan, W. O. *Inorg. Chem.* **1980**, *19*, 165.
(20) Sohrin, Y.; Kokusen, H.; Matsui, M. *Inorg. Chem.* **1995**, *34*, 3928.
(21) Shannon, R. D. *Acta Crystallogr., Sect. A* **1976**, *A32*, 751.
(22) Looney, A.; Han, R.; Gorrell, I. B.; Cornebise, M. Yoon, K.; Parkin, G.; Rheingold, A. L. *Organometallics* **1995**, *14*, 274.
(23) Hartmann, F.; Kläui, W.; Kremer-Aach, A.; Moozt, D.; Strerath, A.; Wunderlich, H. Z. *Anorg. Allg. Chem.* **1993**, *619*, 2071.
(24) Sohrin, Y. Personal communication.
(25) Dailey, B. P.; Shoolery, J. W. *J. Am. Chem. Soc.* **1955**, *77*, 3977.
(26) Levy, G. C.; Lichter, R. L.; Nelson, G. L. *Carbon-13 Nuclear Magnetic Resonance Spectroscopy*; Wiley: New York, 1980 and references therein.
(27) (a) Levy, G. C.; Lichter, R. L. *N-15 Nuclear Magnetic Resonance Spectroscopy*; Wiley: New York, 1979; p 28 ff. (b) Duthaler, R. O.; Roberts, J. D. *J. Phys. Chem.* **1974**, *78*, 2507.

**Table 5.** $^{113}$Cd Chemical Shifts[a] Obtained from Both Solution and Solid State Experiments

| compd | $\delta$ | $\sigma_{iso}$ | $\sigma_{11}$ | $\sigma_{22}$ | $\sigma_{33}$ | $\Delta\sigma$[b] | $\eta$[c] |
|---|---|---|---|---|---|---|---|
| $[B(pz)_4]_2Cd$[d] | 221.1 | 217.7 | 369.9(2) | 250.5(3) | 32.8(4) | −277.3 | 0.65 |
| $[HB(pz)_3]_2Cd$ − a | 198.3 | 207.6 | 330.6(3) | 243.7(2) | 48.5(2) | −238.7 | 0.55 |
| $[Hb(pz)_3]_2Cd$ − b | 198.3 | 177.9 | 303.3(2) | 204.8(1) | 25.7(1) | −228.4 | 0.65 |
| $[B(3\text{-}Mepz)_4]_2Cd$[d] | 202.5 | 188.1 | 296.0(2) | 255.8(3) | 12.5(3) | −263.4 | 0.23 |
| $[HB(3,5\text{-}Me_2pz)_3]_2Cd$[d] | 201.9 | 175.2 | 250.2(5) | 240.3(5) | 35.1(2) | −210.2 | 0.07 |
| $[HB(3\text{-}Phpz)_3]Cd[B(pz)_4]$ | 146.2 | 134.0 | 218.3(7) | 196.8(7) | −13.2(2) | −220.8 | 0.15 |
| $[Hb(3\text{-}Phpz)_3]_2Cd$ | 94.0 | 89.3 | 147.4(5) | 123.4(5) | −3.1(1) | −138.5 | 0.26 |

[a] Positive $^{113}$Cd chemical shifts denote lower shielding than external 0.1 M $Cd(ClO_4)_2$ at 0 ppm. [b] $\Delta\sigma = \sigma_{33} - {}^1/_2(\sigma_{11} + \sigma_{22})$. [c] $\eta = (\sigma_{22} - \sigma_{11})/\sigma_{33} - \sigma_{iso})$. [d] From Lipton, A. S.; Mason, S. S.; Reger, D. L.; Ellis, P. D. *J. Am. Chem. Soc.* **1994**, *116*, 10182.

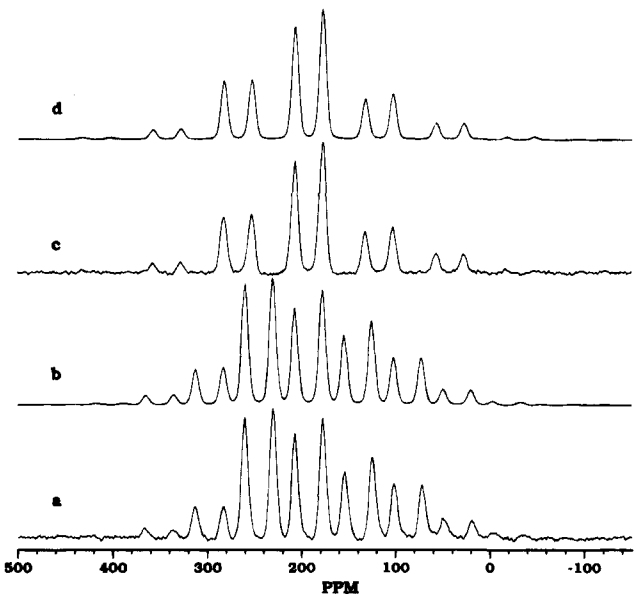


**Figure 7.** Experimental and simulated spectra of $[HB(pz)_3]_2Cd$ (**1**) at two different spinning speeds: (a) experimental spectrum spinning at 3.5 kHz, (b) simulated spectrum of a using 100 Hz Lorentzian and 296 Hz Gaussian line broadening (299 Hz Gaussian for **1b**), (c) experimental spectrum spinning at 5 kHz, and (d) simulation of c utilizing the apodizations described in b.

A correlation of cadmium chemical shifts with nitrogen donor atoms was presented by Summers and Marzilli in 1984.[28] They found that the shifts had the following relationship:

$$\delta = 75A + 51B + 31C \tag{2}$$

where $A$, $B$, and $C$ are the number of primary, secondary, and tertiary amine donors, respectively. The calculated and observed chemical shifts were in good agreement for such species as 1,10-phenanthroline, *N,N,N′,N′*-tetramethylethylenediamine, 2,2′,2″-terpyridine, triethylenediamine, *N,N*-dimethylethylenediamine, and several others.

However, this generalization does not seem to apply well to the family of poly(pyrazolyl)borate ligands. The type of donor nitrogen remains constant, as does the number of coordinating atoms; however, the shifts range from 94.0 to 221.1 ppm. Nonetheless, as the regression analysis shows, the effects of each ligand are additive. There are two basic requirements for the addivity of solution state shifts to work: The first is a fairly constant molecular framework. The second necessity is that the individual tensor elements cannot oppose each other (by moving significantly in opposite directions). To extract the principal components of the shielding tensor we need to look at the solid state NMR data (where the individual components are not averaged).

The addivity model for $^{113}$Cd shielding tensors developed by Honkonen and Ellis[4b] is useful to illustrate the dependencies of the shifts. In that work each tensor element was expanded into a sum of ligand atom contributions in the following way:

$$\sigma_{ii} = \sum_j (\theta_j^m / R_{mj}^3) \cos \phi_j \tag{3}$$

which can be rewritten in a more convenient form to separate out the bonded and nonbonded atoms:

$$\sigma_{ii} = \sum_j (\theta_j^m / R_{mj}^3) \cos \phi_j + \sum_{l \neq j} (\theta_l^m / R_{ml}^3) \cos \phi_l \tag{4}$$

where $\sigma_{ii}$ is the $ii$th element of the shielding tensor, $\theta_j^m$ is a parameter that describes the shielding contribution made by atom $j$ to atom $m$, $R_{mj}$ is the distance between atoms $j$ and $m$, and $\phi_j$ is the angle between the internuclear vector, $R_{mj}$, and the plane orthogonal to the $ii$th component of the shielding tensor. The second summation contains contributions from each nonbonded atom, $l$.

For our six-coordinate species we can rewrite eq 4 using the relation $\lambda_j = \cos \phi_j / R_{jm}^3$ for each nitrogen donor:

$$\sigma_{ii} = \theta_{N_1}\lambda_{N_1} + \theta_{N_2}\lambda_{N_2} + \theta_{N_3}\lambda_{N_3} + \theta_{N_4}\lambda_{N_4} + \theta_{N_5}\lambda_{N_5} + \theta_{N_6}\lambda_{N_6} + \text{nonbonding terms} \tag{5}$$

By collecting terms for each tridentate ligand, we get the following for the individual principal components of the shielding tensor:

$$\begin{aligned} \sigma_{11} &= \theta_{L1}\lambda_{L1}^{11} + \theta_{L2}\lambda_{L2}^{11} + \text{nonbonding terms} \\ \sigma_{22} &= \theta_{L1}\lambda_{L1}^{22} + \theta_{L2}\lambda_{L2}^{22} + \text{nonbonding terms} \\ \sigma_{33} &+ \theta_{L1}\lambda_{L1}^{33} + \theta_{L2}\lambda_{L2}^{33} + \text{nonbonding terms} \end{aligned} \tag{6}$$

One can see that the coordination geometry plays an important part in the shielding environment. The plot in Figure 8 depicts the individual shielding tensor elements for each respective complex and the average Cd−N bond distance. Isotropic shifts obtained from the solution state experiments show the shifts of **1**, **2**, **3**, and **11** to be very similar, with **4** (and the mixed-ligand complexes containing a $[HB(3\text{-}Phpz)_3]^-$ ligand) being much more shielded. However, the data extracted from the CP/MAS experiments show more sensitivity to the coordination geometry, which is expected from the removal of solvent effects, fluxional processes, and other averaging mechanisms. To understand this dependence of the isotropic shift on the bond distance, it is necessary to look at the orientation of the individual tensor elements.

The previous assignment of the most shielded tensor element, $\sigma_{33}$, to be orthogonal to the plane of the nitrogen donor atoms of one ligand followed from the symmetry of **2**.[6] With the presence of an axis of symmetry, the three principal elements of the shielding tensor reduce to $\sigma_\perp$ and $\sigma_\parallel$ (the unique element, $\sigma_{33}$, becomes $\sigma_\parallel$). The similarity of this tensor component in

(28) Summers, M. F.; Marzilli, L. G. *Inorg. Chem.* **1984**, *23*, 521.

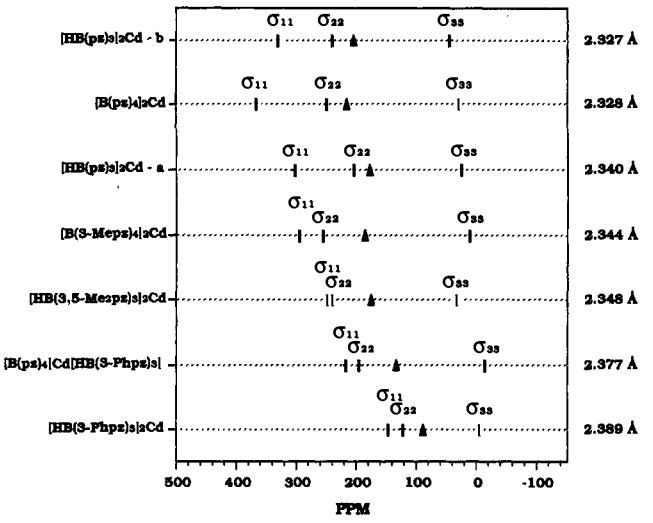


**Figure 8.** Plot of the principal components of the chemical shielding tensor for entire series of six-coordinate complexes, where the individual tensor elements are indicated and the isotropic shifts are represented by the filled triangles.

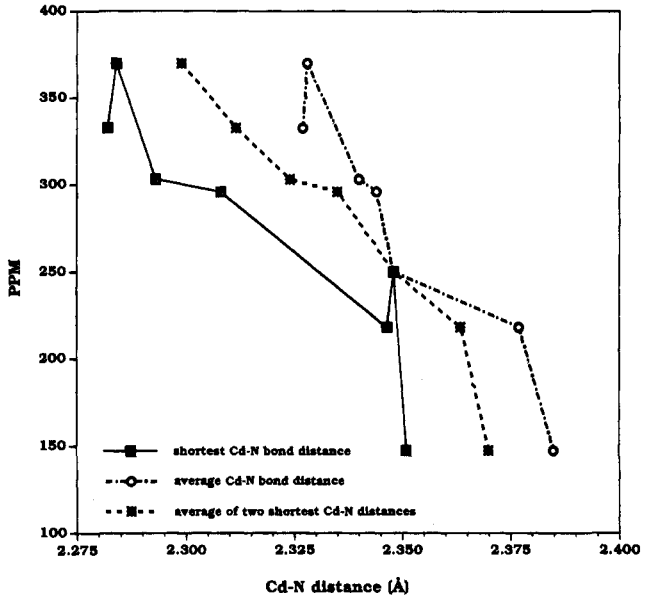


**Figure 9.** Plot of the most deshielded tensor element, $\sigma_{11}$, versus Cd−N bond distances.

$[B(pz)_4]_2Cd$ and $[B(3\text{-}Mepz)_4]_2Cd$ with **2** lent credence to the assignment of this element along the normal of the plane of the coordinating nitrogens of a tridentate chelate. This trend also seems evident in the complexes studied here; as shown in Figure 8, the $\sigma_{33}$ element remains fairly constant for all of the compounds. From previous single crystal results we know tensor elements of like magnitude have similar orthogonal environments,[4] therefore, we assign all of the $\sigma_{33}$ elements to be in nearly the same orientation.

As the $\sigma_{33}$ element is relatively invariant with Cd−N bond distance, it does not account for the isotropic shift tracking the average bond distances. The $\sigma_{11}$ component does however follow the same trend as the isotropic resonance. Figure 9 compares the relationship of $\sigma_{11}$ to the shortest Cd−N bond and the average of all the bond distances. One can see that the shortest bond distance is the dominant influence of the shielding effects. The outlying complex is **3**, which differs from the other compounds studied here in that it has two short Cd−N bonds rather than two long bonds. Another paradigm from the previous single crystal work is that the least shielded tensor element is oriented to maximize the contributions from the shortest bonds. It is therefore reasonable that the $\sigma_{11}$ element for **3** is more deshielded than one would expect (by only looking at the shortest bond).

The dependence of the most deshielded tensor element (and therefore the isotropic shift) upon the cadmium nitrogen bond distances is exactly what one would expect following from eq 4. To modulate the bond distances, all that is needed is to increase (or decrease) the steric effects by changing the substituents in the 3-position of the pyrazolyl ring. Other electronic effects can also be introduced by changing the 5-position of the rings and/or going from a tris ligand to tetrakis. The balance between coordination geometry (and symmetry) and electronic effects remains an important part of our ongoing research. In short, the linear plot depicted in Figure 5 clearly indicates that there is one tensor element, $\sigma_{11}$, that is responsible for the observed trend. Figure 8 completely supports such a conclusion.

## Conclusions

To summarize, we have determined the shielding effects of several poly(pyrazolyl)borate ligands on the cadmium chemical shift. The effects are also seen to depend upon the coordination geometry, primarily the Cd−N bond distances. Minor changes of the substituents of the pyrazolyl ring lead to these coordination changes, which in turn are reflected in the shielding tensors of the cadmium. By utilizing this information, we can now craft or tune ligand systems to mimic systems of interest, i.e., metalloproteins or enzymes. Several studies are now underway to investigate the effects of mixed donor atom combinations upon the cadmium chemical shifts.

**Acknowledgment.** The National Science Foundation (D.J.D., CHE91-19737) and the National Institute of Health (GM-26295) (D.L.R. and P.D.E.) provided financial support. The NSF (Grants CHE-8411172 and CHE-8904942) and NIH (Grant RR-02425) have supplied funds to support NMR equipment, and the NIH (Grant RR-02849) has supplied funds to support mass spectrometry equipment at South Carolina. A.S.L. is supported by the Associated Western Universities, Inc., Northwest Division under Grant DE-FG06-89ER-75522 with the U.S. Department of Energy. A.S.L. and P.D.E. are also supported by Pacific Northwest Laboratory which is a multiprogram national laboratory operated by Battelle Memorial Institute for the U.S. Department of Energy under Contract DE-AC06-76RLO 1830.

**Supporting Information Available:** Tables providing complete listings of atomic coordinates and equivalent isotropic displacement parameters, bond lengths, bond angles, and anisotropic thermal parameters for complexes **1** and **10**, ORTEP views with complete numbering schemes, and included are the CP/MAS spectra and simulations of **4** and **10** (16 pages). This material is contained in many libraries on microfiche, immediately follows this article in the microfilm version of this journal, and can be ordered from the ACS, and can be downloaded from the Internet; see any current masthead page for ordering information and Internet access instructions.

JA951883A